Journal of Crystal Growth 312 (2010) 3603–3608

Contents lists available at ScienceDirect

Journal of Crystal Growth

journal homepage: www.elsevier.com/locate/jcrysgro

Effect of mixing on the crystal size distribution of borax decahydrate in a batch cooling crystallizer

Marija Akrap [a], Nenad Kuzmanić [a,*], Jasna Prlić-Kardum [b]

[a] University of Split, Faculty of Chemistry and Technology, Teslina 10/V, 21000 Split, Croatia
[b] University of Zagreb, Faculty of Chemical Engineering and Technology, Marulićev trg 19, 10000 Zagreb, Croatia

ARTICLE INFO

Article history:
Received 22 July 2009
Received in revised form
24 May 2010
Accepted 8 September 2010
Communicated by J.B. Mullin
Available online 25 September 2010

Keywords:
A1. Solubility
A1. Stirring
A2. Growth from solution
A2. Industrial crystallization
B1. Borates

ABSTRACT

The effect of the impeller speed upon the metastable zone width, supersaturation level, crystal growth and the crystal size distribution of borax decahydrate have been investigated to find operating conditions of a batch cooling crystallizer. The importance of impeller speed was studied in baffled stirred crystallizer with a volume of about 2 dm^3, equipped with four straight blade turbine (4-SBT) cooling at a constant cooling rate. The metastable zone width was determined by visual method, while concentration changes during the process were monitored in line using ion-selective electrode. The crystal size distribution was determined by optical microscope and sieve analysis respectively. The power consumption measurements were performed for all impeller speeds examined as well. On the basis of the experimental results and observations it is evident that in an agitated batch crystallizer the above mentioned parameters are significantly influenced by hydrodynamic regime in the system determined by impeller used and its revolution speed.

1. Introduction

Crystallization is one of the powerful methods for separation and purification in many domains, such as chemical, pharmaceutical and food industries. Agitated vessels are most commonly used equipment in industrial crystallization, and it has been well known that the mixing has dramatic effect on the properties of the product, including crystal size distribution (CSD), purity, morphology and polymorphic form [1,2]. Unfortunately, in many processes of pharmaceutical or chemical industry, crystallizations are carried out in stirred vessels without any optimization of the hydrodynamic conditions, even if, sometimes, these mechanisms are the controlling steps for an efficient separation of the crystals from the liquor and for a suitable morphology of the final product [3].

The purpose of the present work is to investigate the effect of mixing on the borax decahydrate ($Na_2B_4O_7 \times 10\ H_2O$) crystallization in a batch cooling crystallizer. Borax is a product of great industrial interest. It presents the refined form of natural sodium borate used widely in detergent and cleaning formulations, as fungicide, disinfectant or herbicide. It has important role as an agent that modifies the structure of glasses, especially in the production of ultra thin screens, etc. In order to produce crystals of borax with a specified purity and CSD at minimum cost, it is necessary to operate the crystallizer at the optimum mixing conditions [4–6]. Mechanical stirred system equipped with a straight blade turbine (4-SBT) in the vessel with a flat bottom was used during experimental procedure. Different impeller speeds were adopted in batch crystallization, and the effect upon the size distribution of the product crystals was investigated thoroughly.

2. Experimental procedure

The experimental set-up is shown schematically in Fig. 1. All experiments were performed in a laboratory-scale stirred batch cooling crystallizer with a volume of 2 dm^3. The crystallizer was the cylindrical flat bottom vessel with internal diameter of 0.14 m. The vessel was fitted with four baffles placed at 90° around the vessel periphery. The baffle widths were equal to one-tenth of vessel diameter ($d_T/10$). The solution was stirred by straight blade turbine ($D/d_T=0.45$; number of blades—4; blade width—0.12D). The clearance of the impeller from the tank bottom was fixed to $C=1/3H$. Temperature control of the crystallizer was accomplished by a programmable thermostatic bath (Huber Compatible Control CC 3) with a temperature control accuracy × 0.01 °C and data acquisition system. All experiments were carried out at the constant cooling rate of 6 °C h^{-1}. During the process concentration changes of borax solution were monitored in line using Na-ion selective electrode (ISE). The measurements were restricted to temperature below 35 °C in order to avoid any decomposition phenomena and problems

* Corresponding author.
E-mail address: kuzmanic@ktf-split.hr (N. Kuzmanić).

0022-0248/$ - see front matter © 2010 Elsevier B.V. All rights reserved.
doi:10.1016/j.jcrysgro.2010.09.023

Nomenclature

C	off-bottom clearance (m)
c	solution concentration (mol dm^{-3})
c^*	solubility (mol dm^{-3})
Δc	supersaturation (mol dm^{-3})
Δc_{max}	maximum supersaturation (mol dm^{-3})
x	particle size (μm)
x_m	mean particle size defined by Eq. (4) (μm)
d_T	tank diameter (m)
D	impeller diameter (m)
H	height of liquid from tank bottom (m)
l	radial sampling position from the tank wall (m)
m	suspension mass (kg)
N	impeller speed (rps or rpm)
$Q_r(x)$	cumulative frequency function (−)
r	type of quantity of particles (r=0—particle number; r=3—mass or volume of particle)
(P/m)	power consumption per unit mass (W kg^{-1})
t	process time (min)
T	temperature (°C)
T_s	saturation temperature (°C)
Y	product yield (wt%)
ΔT_{max}	maximum available undercooling (°C)
z	axial sampling position from the tank bottom (m)
ρ_L	density of suspension (kg m^{-3})
σ	standard deviation defined by Eq. (5) (−)

connected with operating mode of ISE as well. The power consumption was determined using torque meters produced by Lightnin-LabMaster. After crystallization for a definite time, the crystals were filtered from the residual solution, and then were dried overnight in air at room temperature in order to measure crystal size distribution. The crystal size distributions were determined by sieve analysis and optical microscope.

2.1. Measurement of solubility

The solubility of borax was determined in the range from 3 to 35 °C. Saturated borax solutions were prepared by dissolving analytically pure borax decahydrate in ultrapure water. A flask containing the saturated solution and excess solid phase of borax was put into a thermostatically controlled bath, and was stirred for 6 h to attain equilibrium. After attaining saturation, the equilibrium concentration of borax was determined by volumetric titration with NaOH in the presence of mannitol and phenolphthalein as indicators [7].

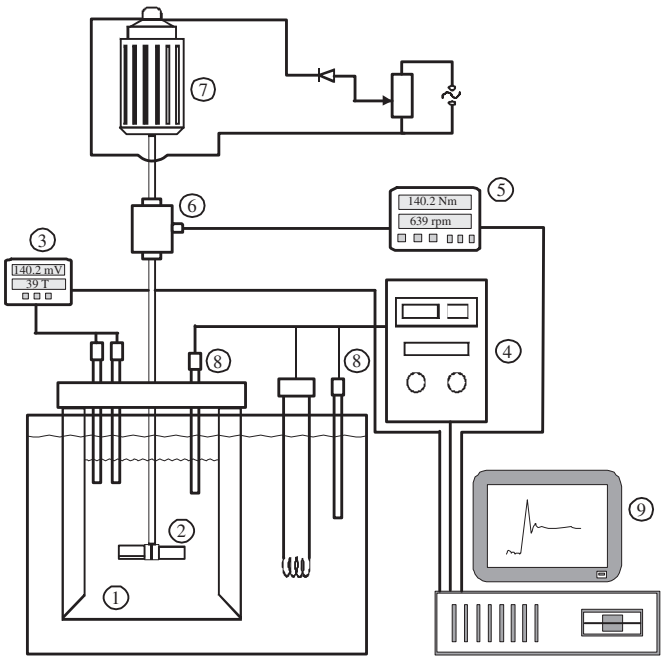

Fig. 1. Experimental set-up: (1) crystallizer, (2) impeller, (3) system for concentration measurement, (4) programmable thermostat, (5) torquemeter, (6) torque sensor and velocity transducer, (7) variable speed motor, (8) temperature probes and (9) computer.

2.2. Measurement of metastable zone width

The metastable zone widths of borax solutions were measured by the conventional polythermal method [8]. A solution with known composition was prepared in accordance with solubility data. The saturated solution was cooled down at a given linear cooling rate until the shower of visible nuclei appeared. Then, this method consists in the determination of the maximum undercooling ΔT_{max}

$$\Delta T_{max} = T_s - T_p \tag{1}$$

where T_s is saturation temperature and T_p is temperature at which the first nuclei have been observed. The difference between these two temperatures is called metastable zone width. The relation of maximum supersaturation to the maximum undercooling can be expressed by the following equations [9,10]:

$$\Delta c_{max} = \left(\frac{dc^*}{dT}\right)\Delta T_{max} \tag{2}$$

2.3. Measurement of growth rate and crystal size distribution

During the crystallization, the crystal slurry was withdrawn from the crystallizer in order to estimate the variation of crystal size against elapsed process time. Slurry was withdrawn using a special type of syringe, always from the same place. Sampling point was located above the impeller plane (z/H=0.8; $l/(d_T/2)$=0.4), in the middle plane between adjacent baffles. The withdrawn samples of crystals were sized immediately by microscopy technique with an image analyzer (Motic Images Plus 2.0) in order to investigate the effect of the impeller speed on the overall crystal growth rate.

The size distributions of final products of crystallization were determined by sieve analysis. Sieving of dry solid sample was performed with sieves of 45–300 μm aperture. Experimentally determined CSD is also presented by well-defined mathematical law. Gauss-normal distribution (*GN*) has been found very useful in describing particulate systems analyzed in this work. The expression representing *GN* function on a weight basis is [11,12]

$$\frac{dQ_3(x)}{dx} = \frac{1}{\sigma\sqrt{2\pi}}\exp^{-(x-x_m)^2/2\sigma^2} \tag{3}$$

In Eq. (3), the mean size is defined as

$$x_m = \frac{\Sigma x \Delta Q_3(x)}{\Sigma \Delta Q_3(x)} \tag{4}$$

and standard deviation, σ, is defined as

$$\sigma = \sqrt{\frac{\Sigma (x-x_m)^2 \Delta Q_3(x)}{\Sigma \Delta Q_3(x)}} \tag{5}$$

3. Results and discussion

3.1. Solubility and metastable zone width

Solubility is a very important thermodynamic parameter to determine the crystallization mode, supersaturation, phase diagram and yields. It can also affect the kinetic of crystallization, the particle size distribution and shape, which are controlled by the supersaturation. For a batch cooling crystallization, which is widely used in the production of fine chemicals, the solubility and metastable zone width must be known in order to interpret the mechanism of crystallization [13]. The solubility data, measured over the temperature range from 3 to 35 °C, are plotted in Fig. 2. As shown in this figure, the solubility of borax increases with increase in temperature. Since the solubility depends strongly on temperature, cooling mode is desirable for crystallization of borax. The solubility curve can be approximately described by polynomial function:

$$c^* = 2\times10^{-6}T^3 + 4\times10^{-6}T^2 + 2.6\times10^{-3}T + 0.06 \quad (6)$$

Solubility data obtained in this work are in very good agreement with those reported in the literature [14]. Maximal deviation from literature results in examined temperature range was approximately 2%.

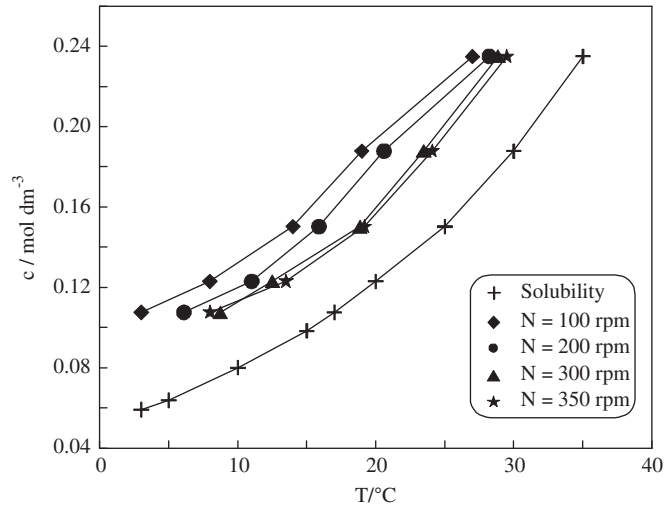

Fig. 2. Borax solubility curve and changes of metastable zone width with impeller speed.

The variations of metastable zone width with saturation temperature for all the impeller speeds examined are also presented in Fig. 2. Since determination of metastable zone width using visual method is highly subjective each experiment was repeated at least three times to ensure reproducibility. T_p is taken as mean arithmetic value with standard deviation of $\times$ 0.37 °C. This deviation was more pronounced at lower saturation temperature.

The experimental results confirm the well known effects of impeller speed on the metastable zone width. It is evident that increment of the impeller speed, that is higher turbulence level in the system (Re_m=7765–27170) causes the metastable zone width to be narrower. Since onset of nucleation is followed by concentration changes, the metastable zone width could also be determined by temperature at which concentration start to decrease (T_p). However, the metastable zone width determined this way is broader for 0.35 °C in average. This deviation is more pronounced at lower impeller speed and lower temperature, when deviation may excide 1 °C. This deviation is direct consequence of ion selective electrode signal delay in detecting of the small changes in concentration at the beginning of nucleation.

Concentration, solubility and supersaturation profiles against process time are presented in Fig. 3. By this way it is possible to visualize how concentration and solubility changes resulting supersaturation profiles at the different impeller speed. The concentration profiles illustrate that overall concentration level tends to decrease when mixing intensity is increased. The supersaturation profile in a batch crystallizer has a profound effect on the nucleation and growth processes, and the resulting CSD as well.

Fig. 3 shows supersaturation profiles in batch crystallization experiments at different impeller speeds. At t=0, the batch crystallizer is filled with a just-saturated solution that contains crystals with a negligible area. The solution begins to supersaturate at a constant rate, and the supersaturation increases until it reaches the limit of the metastable zone (Δc_{max}). At this point, nucleation starts and crystals with a certain surface area begin to form. The increase in total surface area due to nucleation and crystal growth would remove more and more of this supersaturation until, at the end of the batch, the supersaturation decreases to the final value.

3.2. Crystal size distribution

In order to investigate the effect of the impeller speed on the overall crystal growth rate, the samples of crystal suspension were withdrawn and analyzed by an optical microscope and an appropriate image analyzer at different time intervals during the

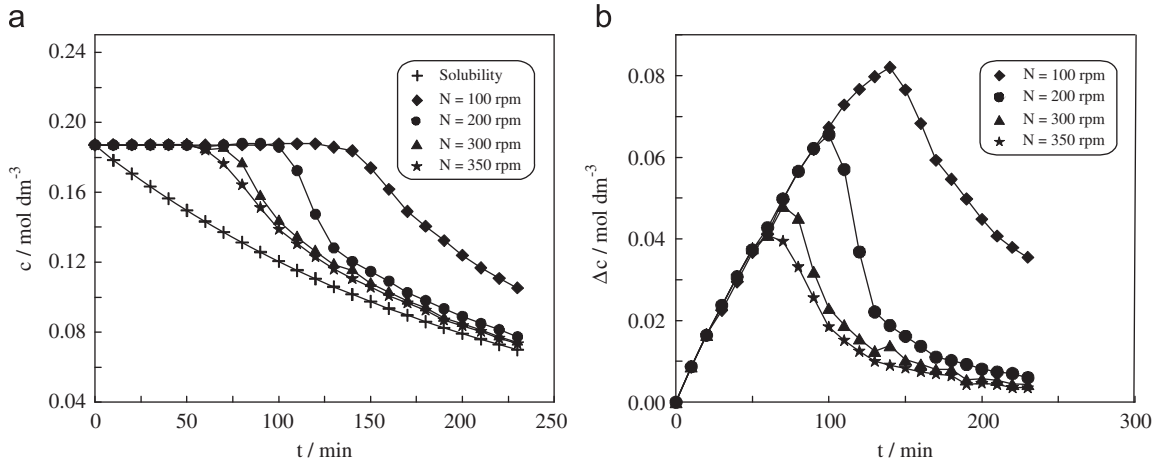

Fig. 3. Concentration and solubility profiles (a) and supersaturation profiles (b) for different impeller speeds.

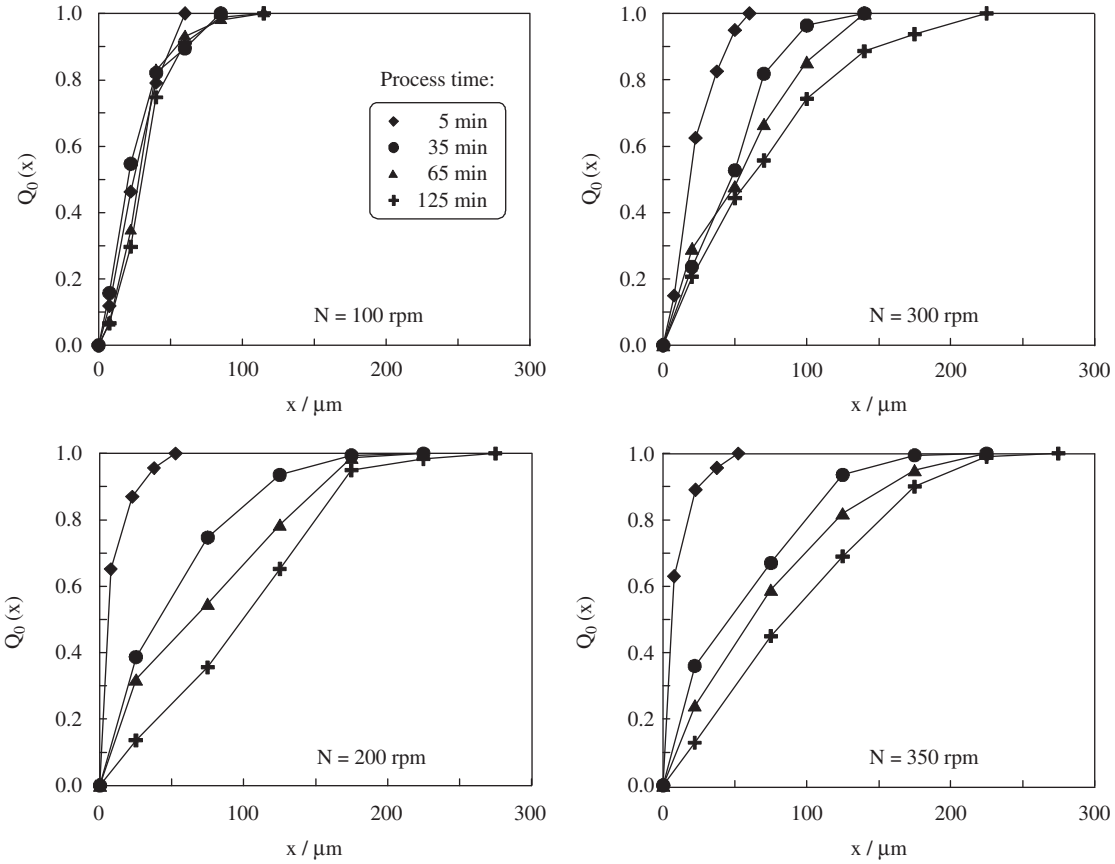

Fig. 4. Cumulative undersize distributions of borax crystals at different process times for various agitation speeds.

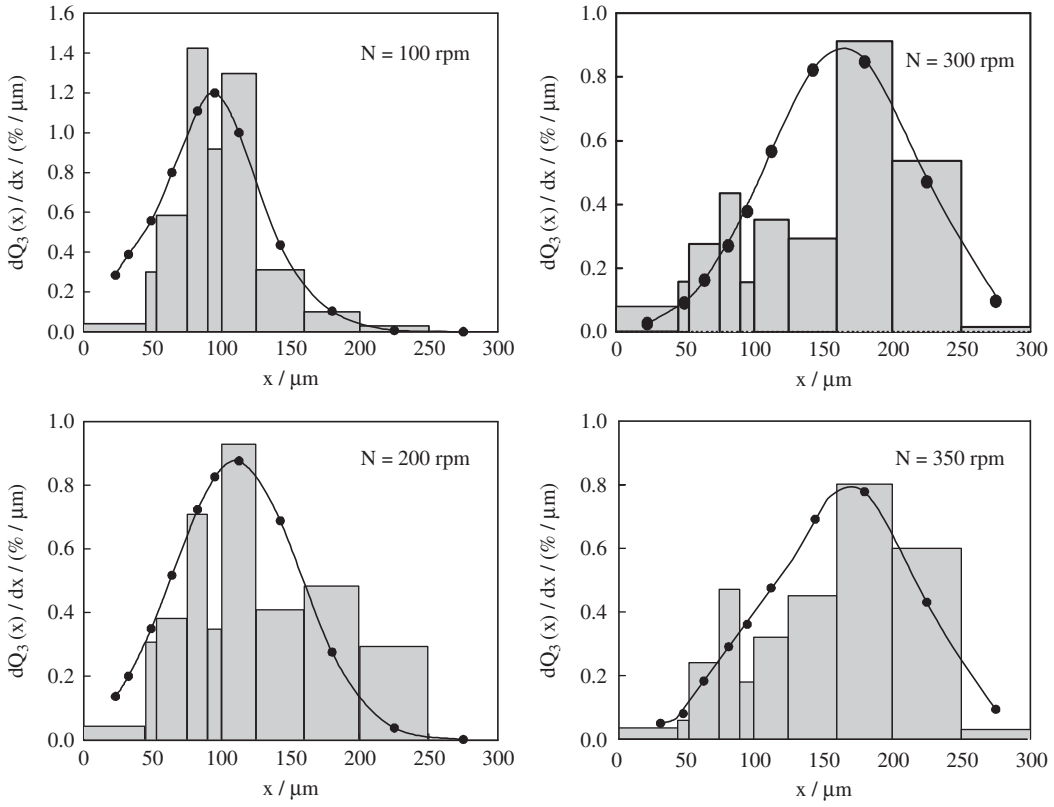

Fig. 5. Fitted (curve) and experimental crystal size distribution (histogram) depending on the impeller speed.

crystallization. The time evolutions of the cumulative size distributions obtained are shown in Fig. 4.

The curves of successive cumulative distribution presented, clearly show that during the crystallization the crystals become larger, however the overall crystal growth rates are different for different impeller speeds. The more pronounced crystal growth have been observed at higher impeller speeds, while at $N=100$ rpm could be noticed certain deviations in cumulative distributions. These deviations are consequence of hydrodynamic conditions, which exist in the crystallizer. Namely, in this case the state of complete suspension has not been achieved [15]. The crystals collect at the bottom of the crystallizer, so there is little crystal surface exposed to the supersaturated solution. In such situations, the process of crystal growth is retarded, that is disabled and the final mother liquor may retain appreciable supersaturation what can be seen from Fig. 3. This fact also affects the CSD of final product obtained at $N=100$ rpm.

The size distributions of final crystal products obtained at different impeller speeds are presented in Fig. 5.

As can be seen from the figure, two maxima in size distributions, i.e. two subdistributions were observed at all examined conditions. The dominant sizes of CSD move toward coarser fractions as impeller speed increases. It indicates that at higher impeller speeds the hydrodynamic conditions are more suitable for crystal growth. In this case, the agitation conditions provided the state of complete suspension of crystal particles and the maximum surface area of the crystals is exposed to the solutions for mass transfer. The second maximum of distributions, that is the maximum at finer sizes is likely inferred to be due to agglomeration and secondary nucleation. Presence of fines in all distribution indicates that secondary nucleation take palace even at the final stage of the process. At lower impeller speed secondary nucleation is consequence of high supersaturation level. At higher impeller speed it is also consequence of crystal breakage, which is caused by collision between crystals and walls of the crystallizer, impeller or other crystal. Crystals produced at higher impeller speed are more regular, regardless of the fact that at these conditions the crystal shape is affected by attrition due to their higher collision probability. The photographs of the final crystals of borax obtained at various agitation speeds made by optical microscope are given in Fig. 6.

Statistical analyses of these experimental distributions show that they follow well-known mathematical low. They can be presented by *GN* distribution function, as presented in Fig. 5. Further, the crystal mean size and standard deviation on the basis of the *GN* distribution are presented in Fig. 7.

The mean crystal size increases with increase in impeller speed, which confirms that higher degree of homogeneity of the suspension is a more suitable option for the crystal growth. At the same time, the calculated values of standard deviations (if we neglect CSD obtained at $N=100$ rpm due to prominent state of uncompleted suspension) indicates that macromixing affects the width of CSD. This effect is not so pronounced, but regardless of all it could not be neglected.

The product yields, expressed as wt% of the solid at the end of each of crystallization run, are also presented in Fig. 7. Results illustrate that the product yield increases with increment of impeller speed, but at $N \geq 200$ rpm this parameter tends to obtain an asymptotic value.

3.3. Power consumption

Generally, the power consumption is defined as the quantity of energy input to the liquid phase by stirrer per unit time. Proper choice of hydrodynamic conditions in an agitated vessel may considerably facilitate and improve the process of crystallization. The choice closely depends on the knowledge of the power consumption as well. In this work the power input of the impeller

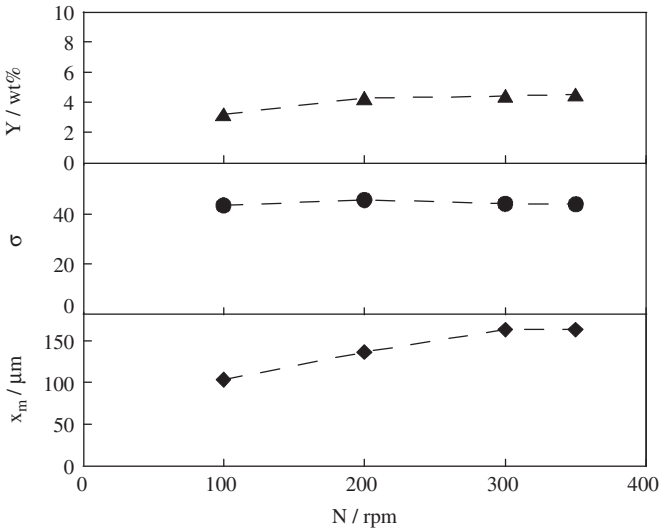

Fig. 7. Product yield, standard deviation and mean crystal size for different impeller speeds.

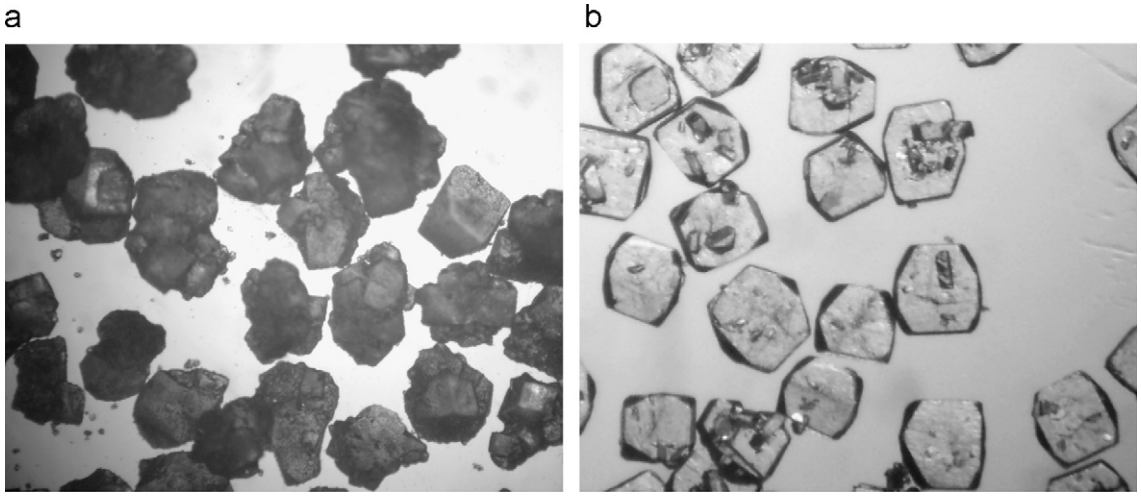

Fig. 6. The photographs of borax crystals obtained at various agitation speeds (a) $N=100$ rpm and (b) $N=350$ rpm; $T_s=30$ °C.

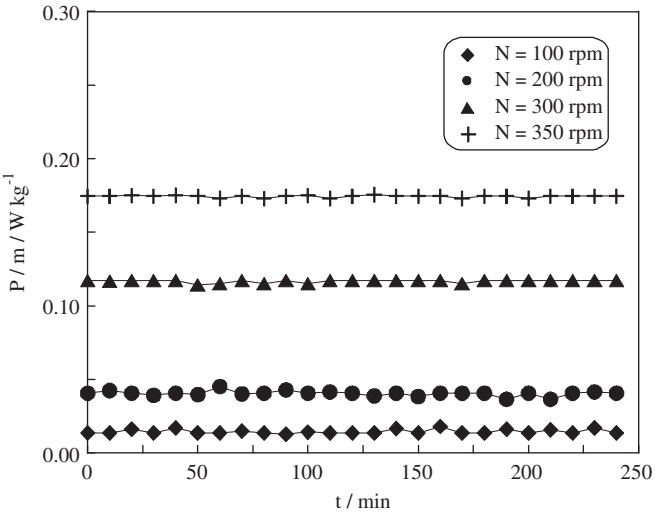

Fig. 8. Power consumption per unit mass of suspension versus process time for various agitation speeds.

used was calculated from the torque and the impeller speed and it is expressed in terms of power consumption per unit mass of suspension. Because of the difficulty in establishing the real density of the agitated suspension, the liquid density, has been adopted as the reference value ($\rho_{L,30\,^{\circ}C}$=1029 kg m^{-3}). For solid/liquid systems, especially when solid loading is relatively low, this approach has been traditionally accepted [16,17]. The torque measurements were performed for all impeller speeds examined.

From Fig. 8, it can be seen that values of power consumption per unit mass of suspension increased with increase in impeller speed. Since the crystallization is process in which a new, solid phase forms from supersaturated solution, a data acquisition software package was used to evident the possible changes of power consumption during the process. The obtained results also indicated that values of this parameter do not change over the process time regardless of the fact mentioned above. Obviously, presented results cannot be taken for granted, because experiments in this work were carried out in crystallizer of relatively small volume. These effects should be studied further in greater detail employing experimental units of larger scale, since for the scale-up of crystallization process the power input is of fundamental interest.

4. Conclusions

In an agitated batch crystallizer, metastable zone width, crystal growth as well as crystal size distribution are significantly influenced by hydrodynamic regime in the system determined by impeller used and its rotational speed.

The successive cumulative distribution functions determined during the process clearly show that the overall crystal growth rates are different for different impeller speeds. The more pronounced crystal growth has been observed at higher impeller speed, while at N=100 rpm could be noticed certain deviations in cumulative distributions due to the state of uncompleted suspension of crystal produced during the process.

The size distributions of the final crystal products obtained at all examined conditions are characterized by two maxima. The dominant sizes of CSD move toward coarser fractions as impeller speed increases. It indicates that higher impeller speed causes the more suitable hydrodynamic conditions in the system regarding crystal growth. The maximum at finer sizes is inferred to be due to agglomeration and secondary nucleation. Statistical analyses of these experimental distributions show that they can be well presented by *GN* distribution function. The mean crystal size increases with increase in impeller speed, while the values of standard deviation indicate that macromixing affects the width of CSD. This effect is not so pronounced, but regardless of all it could not be neglected.

In the examined system the power consumption per unit mass of suspension increased with increase in impeller speed. The obtained results also indicated that the values of this parameter are nearly constant over time, so they do not change during the process of crystallization regardless of the fact that during the process the new solid phase forms.

References

[1] A.S. Myerson, in: Handbook of Industrial Crystallization, first ed., Butterworth-Heinemann, Boston, 1993, pp. 33–63.
[2] E.L. Paul, V.A. Atiemo-Obeng, S.M. Kresta, Handbook of Industrial Mixing—Science and Practice, first ed., John Wiley & Sons, Inc., New Jersey, 2004, pp. 1057–1069.
[3] L. Marmo, L. Manna, F. Chiampo, S. Sicardi, G. Bersano, Influence of mixing on the particle size distribution of an organic precipitate, J. Cryst. Growth 166 (1996) 1027–1034.
[4] K. Shimizu, H. Nagasawa, K. Takahashi, Effect of off-bottom clearance of a turbine type impeller on crystal size distribution of aluminum potassium sulfate in a batch crystallizer, J. Cryst. Growth 154 (1995) 113–117.
[5] K. Shimizu, T. Nomura, K. Takahashi, Crystal size distribution of aluminum potassium sulfate in a profiled, a dished, or a flat bottom crystallizer equipped with a pitched paddle, J. Cryst. Growth 191 (1998) 185–189.
[6] K. Shimizu, K. Takahashi, E. Suzuki, Effect of baffle geometries on crystal size distribution of aluminum potassium sulfate in a seeded batch crystallizer, J. Cryst. Growth 197 (1999) 921–926.
[7] R.S. Braman, Boron determination, in: F.D. Snell, F.D. Hilton (Eds.), Encyclopedia of Industrial Chemical Analysis, vol. VII, Interscience Publisher, New York, 1968, pp. 405–409.
[8] J. Ulrich, C. Strege, Some aspects of the importance of metastable zone width and nucleation in industrial crystallizers, J. Cryst. Growth 237–239 (2002) 2130–2135.
[9] H. Gurbuz, B. Ozdemir, Experimental determination of the metastable zone width of borax decahydrate by ultrasonic velocity measurement, J. Cryst. Growth 252 (2003) 343–349.
[10] J.W. Mulin, in: Crystallization, fourth ed., Elsevier, Amsterdam, 2004, pp. 180–215.
[11] A. Vrhunec, A. Kolenc, D. Teslič, I. Livk, C. Pohar, Crystal size distribution in batch sodium perborate precipitation, Acta Chim. Slov. 46 (4) (1999) 543–554.
[12] T. Allen, Particle Size Measurement, fifth ed., Chapman&Hall, London, 1997, pp. 74–112.
[13] K.J. Kim, A. Mersmann, Estimation of metastable zone width in different nucleation processes, Chem. Eng. Sci 56 (2001) 2315–2324.
[14] 〈http://www.borax.com〉.
[15] N. Harnby, M.F. Edwards, A.W. Nienow, Mixing in the Process Industries, second ed., Butterworth-Heinemann, Oxford, 1997, pp. 364–392.
[16] K.L. Harrop, W.H. Spanfelne, M. Jahoda, N. Otomo, A.W. Etchelles, W. Bujalski, A.W. Nienow, Impact of Suspended Solids on the Homogenisation of the Liquid Phase under Turbulent Conditions in a Stirred Vessel, Recents Progres an Genie des Procedes 11 (52) (1997) 41–48.
[17] K.S.M.S. Raghav Rao, J.B. Joshi, Liquid-phase mixing and power consumption in mechanically agitated solid-liquid contactors, Chem. Eng. J. 39 (1988) 111–124.